Journal of Molecular Liquids 258 (2018) 335–344

Contents lists available at ScienceDirect

Journal of Molecular Liquids

journal homepage: www.elsevier.com/locate/molliq

Experimental and modelling study on strontium removal from aqueous solutions by *Lagenaria vulgaris* biosorbent

Milan Z. Momčilović [a,*], Antonije E. Onjia [b], Dragana N. Trajković [a], Miloš M. Kostić [c], Dragan D. Milenković [d], Danijela V. Bojić [c], Aleksandar Lj. Bojić [c]

[a] University of Belgrade, "Vinča" Institute of Nuclear Sciences, 11000 Belgrade, Serbia
[b] University of Belgrade, Faculty of Technology and Metallurgy, 11000 Belgrade, Serbia
[c] University of Niš, Faculty of Sciences and Mathematics, 18000 Niš, Serbia
[d] High Chemical Technological School, 37000 Kruševac, Serbia

ARTICLE INFO

Article history:
Received 17 January 2018
Received in revised form 12 March 2018
Accepted 13 March 2018
Available online 16 March 2018

Keywords:
Strontium
Pollution
Sorption
Lagenaria vulgaris
Biosorbent

ABSTRACT

The shell of *Lagenaria vulgaris* (LV) plant was used as biosorbent for strontium removal from aqueous solutions. Chemical structure of the biosorbent's surface was characterized by the means of FTIR and Boehm's titrations. SEM-EDX technique was used to study the morphology and elemental composition of the material. The analyses pointed out to abundance of acidic functional groups which are charged in solution and hence responsible for ionic exchange of Sr(II) ions. Sorption was examined by varying initial concentrations of Sr(II) in solutions, sorbent's loadings, pH, and contacting times. Equilibrium of the process was attained in the first 10 min of contacting and followed pseudo-second order and Chrastil's kinetic models. It was established that sorption onto aLVB was heterogenous by nature and fitted well to Freundlich and Sips isotherm models with maximum sorption capacity of 29.55 mg g^{-1}. Sorption potentail was kept high after six cycles when acidic desorbents were used.

1. Introduction

The treatment of radioactive wastewater containing ^{90}Sr has received great attention especially after the tragedy of Fukushima Daiichi, Japan in 2011. Also, it is established that strontium contamination in groundwater and other water sources is the threat that requires concern and action. Strontium isotope 90 is the principle medium lived fission product with half-life of 28.8 years [1]. It is being released into the environment by the nuclear weapon testing, uncontrolled discharge of waste effluents from nuclear reactors and nuclear fuel reprocessing, by accidental release [2], etc. Due to its long life span, high solubility, its bio-toxicity [3], high transferability, and easy accumulation in terrestrial and aquatic organisms [4,5], separation and recovery of this ion from contaminated water sources needs special attention in the field of environmental science and technology.

Although many physico-chemical techniques have been tested for removal of radioactive metal ions from aquaeous media including solvent extraction [6], reduction [7], chemical precipitation [8], membrane filtration [9], immobilizations [10], vacuum membrane distillation [11], only sorption imposed as an economic and efficient solution for this task. Various types of sorbents were utilized for removal of strontium ions from aqueous media such as: activated carbons [12], zeolites [13], carbon nano tubes [14], hydroxyapatite [15], manganese antimonate [16], dolomite powder [17], etc. In addition, some biosorbents showed great potential, especially yeasts [18,19], mosses [20], bacteria [21] and roots of plants [22].

Lagenaria vulgaris (Cucurbitaceae) is a creeping, hardy plant found growing mainly on alluvial sandy soil and red loam, in flat areas and moderate slopes, on light and warm terrains [23]. Its characteristic gourds are harvested young and used as a vegetable or it is harvested mature, then dried, and it is mostly used for making water containers and decorations. The outer shell of the gourd is hard and ligneous while the inside is a spongy white pith of bitter taste. Although it is indigenous to Africa, LV plant is often grown in Serbia.

In this study, the ability of biosorbent based on LV shell to remove ions of naturally stable isotope of strontium from aqueous solutions was examined. For safety reasons, this isotope was taken instead of radioactive ^{90}Sr considering similar chemical reactivity for both isotopes [24]. The sorption processes were examined in batch system by considering effects of contact time, pH of the suspensions and initial metal ions concentration. Kinetics and equilibrium study was interpreted by using several theoretical models. The results are represented in comparable and useful fashion followed by instructive conclusions of great significance for practical fields of strontium removal.

* Corresponding author at: "Vinča" Institute of Nuclear Sciences, University of Belgrade, P. O. Box 522, 11001 Belgrade, Serbia.
E-mail address: milanmomcilovic@yahoo.com (M.Z. Momčilović).

https://doi.org/10.1016/j.molliq.2018.03.048
0167-7322/

2. Materials and methods

2.1. The sorbent

The shells of *Lagenaria vulgaris* originate from the plant grown in the southern Serbia at an altitude of 700 m with irrigation and without fertilization. Raw *Lagenaria vulgaris* shells were air dried, washed with distilled water and grounded. This grounded biomass was soaked in 0.3 M HNO_3 for 24 h. The acid treated material was washed with a deionized water to remove excess of acid and stirred on a magnetic stirrer with 0.1 M NaOH for 30 min. The neutralized biomass was washed again with deionized water and dried in an oven at 55 ± 5 °C. Particles in sizes from 0.4 to 0.8 mm were collected by sieving and were used for all the experiments. This material was designated as aLVB [25].

2.2. FTIR

Fourier transform infrared spectroscopy (FTIR) analysis was used to determine characteristic functional groups present on the surface of aLVB. For this purpose, FTIR spectrometer Bomem MB-100 (Hartmann & Braun, Canada) was operated in spectral range 4000–400 cm^{-1} with resolution of 2 cm^{-1}. The sample was compressed in a potassium bromide pellet prior to spectroscopy.

2.3. SEM and EDX study

For scanning electron microscopy, microscope JSM-6610 LV (Jeol, Japan) was used. Before the analysis, the biosorbent sample was dried at 110 °C for 4 h. After this, a thin layer of gold was deposited on the surface of the sample by evaporation at the distance of 50 mm from the source for 180 s in evaporator SCD005 (Leica Microsystems, Germany). The degree of magnification was correlated to the various diameters of the areas of interest which was in the range from 25 to 40 nm. Although various magnifications were used to explore the surface, only representative images at the magnification of 500 times are presented. The EDX technique was used to determine the elemental composition of the biosorbent before and after strontium uptake. EDS detector model X-Max Large Area Analytical Silicon Drift connected to INCAEnergy 350 Microanalysis System was used.

2.4. pH_{pzc}

Point of zero charge (pH_{pzc}) was determined by the pH drift method. It is defined as the pH value of suspension at which surface of the suspended matter has no charge. For this analysis, 0.01 M KNO_3 was used as a supporting inert electrolyte. The pH values of the tested solutions were adjusted in the range between 2 and 10 by using 0.01 M HNO_3 and 0.01 M KOH. Then, 0.2 g of biosorbent was introduced to series of glass tubes which contained 50 cm^3 of test solutions at different initial pH values (pH_i) and equilibrated for 24 h. The final pH values (pH_f) of suspensions were measured after 24 h and plotted against the initial pH. The pH value at which $pH_i = pH_f$ was taken as pH_{pzc}. pH was measured by SensIon3 (Hach, USA) which was calibrated before every run.

2.5. Boehm titrations

Boehm's method is used to quantify carboxylic, lactonic and phenolic functional groups on the surface of the analyzed powder material in aqueous suspensions. Differences in acidity of these functional groups are exploited for selective neutralization by the bases of different strength (NaOH, $NaHCO_3$, Na_2CO_3). Prior to the beginning of this process, each biosorbent was protonated with 0.01 M HCl, filtered and dried at 50 °C. Then, 0.5 g of protonated biosorbent was suspended in 50 cm^3 of 0.1 M $NaNO_3$ as a supporting electrolyte. In order to achieve equilibrium, the suspension was stirred on a magnetic stirrer for 90 min and then filtered. Titrations were carried out with the bases of different strength, bearing in mind that NaOH neutralizes all acidic functional groups on the surface of the sorbent, Na_2CO_3 neutralizes carboxylic and lactonic, while $NaHCO_3$ neutralizes only carboxylic functional groups. Increments of bases (0.04–0.06 cm^3) were slowly added. Endpoint of titration was determined by using an indicator. In order to avoid dissolution of carbon dioxide from the air in the solution, titrations were carried out while gaseous nitrogen of high purity was bubbled into the suspensions.

2.6. Reagents

Commercial strontium nitrate which contained a mixture of strontium isotopes with the average atomic number 87.62 was used. Solutions of strontium (II) were prepared by dissolving analytical grade of $Sr(NO_3)_2$ purchased from Sigma-Aldrich in deionized water to the concentration of 1000 mg dm^{-3}. This stock was used to prepare Sr(II) solutions in concetrations from 50 to 400 mg dm^{-3}. For all the experiments, water of 18.2 MΩ obtained in laboratory from the demineralizator Smart2Pure (Thermo, USA) was used.

2.7. Batch sorption studies

Biosorption of Sr(II) ions was done in a batch system. The effects of time, pH, initial strontium concentration and dosage of sorbent were studied. The impact of pH was investigated in the range from 2 to 10. It was adjusted by either 0.1 M HNO_3 or 0.1 M NaOH solutions at the beginning of the contacting and controlled during the experiments. The effects of initial Sr(II) concentration were investigated for the following concentrations: 10, 20, 50, 100, 200, 400, and 800 mg dm^{-3}. The experiments were conducted in 250 cm^3 Erlenmeyer flask with a magnetic stirring. Aliquots of 5 cm^3 were collected after 0, 1, 2, 4, 10, 20, 40, 60, 90, 120 and 240 min in order to examine kinetics. The amount of sorbed strontium was determined from the difference between the initial and final concentrations of Sr(II) in solutions by the means of atomic absorption spectroscopy by using spectrometer model AAnalyst 400 (Perkin-Elmer, USA).

The sorption capacity of the sorbent was calculated by the following equation:

$$q = (c_i - c_t)V/m \tag{1}$$

where q is the sorption capacity (mg g^{-1}), c_i is the initial strontium concentration (mg dm^{-3}), c_t is the strontium concentration in solution (mg dm^{-3}) after time t, m is the mass of sorbent used (g), and V is volume of the solution (dm^3).

For the case of sorbent's dosage, the removal efficiency was calculated by the equation:

$$R(\%) = \frac{(c_i = c_e)}{c_i} \cdot 100 \tag{2}$$

where c_e is the equilibrium concentration of Sr(II).

To ensure the accuracy, reliability, and reproducibility of the collected data, all the experiments were carried out in triplicate and mean values were recorded. The results were represent as mean values ± SD.

The standard deviation from the means was calculated by using the equation:

$$SD = \sqrt{\cdot \frac{\sum_{i=1}^{n}(x_i - \bar{x})^2}{n-1}} \cdot \frac{\sum_{i=1}^{n}(x_i - \bar{x})^2}{n-1} \; SD = \sqrt{\cdot \frac{\sum_{i=1}^{n}(x_i - \bar{x})^2}{n-1}} \tag{3}$$

where: n – the number of experimental data points, x_i – the value of the individual data point, $\bar{x}$ – the average of the data points.

2.8. Desorption of Sr(II) and regeneration of aLVB.

For the desorption study, 1 g of aLVB was loaded with 250 cm^3 of Sr (II) solution with concentration of 50 mg dm^{-3} and stirred for 240 min. Then, aLVB was separated by filtration and concentration of Sr(II) was determined in filtrate. Separated biomass was gently washed with deionized water to remove strontium retained in the structure. After that, biosorbent was contacted with 100 cm^3 of desorbent solutions: 0.1 M HNO_3, 0.1 M HCl or 0.1 M NaCl. The suspensions were stirred for 120 min, then the filtrates were analyzed to determine the concentration of Sr(II) ions after desorption. Desorption efficiency (DE%) was calculated by using the equation:

$$DE\% = \frac{m_{de}}{m_{sr}} \times 100 \quad (4)$$

where m_{de} is the mass of desorbed strontium, and m_{sr} is the mass of previously sorbed strontium.

After desorption, biosorbent was separated from the desorbent solution and washed with deionized water. It was reconditioned (deprotonated) by being treated with 0.01 M NaOH solution and washed thoroughly with deionized water until the neutral pH. The metal-desorbed biosorbent was used as the regenerated material in five repeated sorption-desorption cycles in order to estimate its reusability.

3. Results and discussion

3.1. FTIR analysis

Presence of functional groups in aLVB sample is clearly represented by FTIR spectrum given in Fig. 1. The broad and intense peak at 3429 cm^{-1} originates from the stretching of O—H bonds due to inter- and intra-molecular hydrogen bondings. These bondings refer to alcohols, phenols, and carboxylic acids present in the cellulose and lignin which are the main constituents of aLVB. The peaks at 1653 and 1636 cm^{-1} probably originate from C═O stretching vibrations. The distinctive band at 2924 cm^{-1} corresponds to symmetric or asymmetric C—H stretching vibration of aliphatic acids. The peak detected at 1733 cm^{-1} is from stretching vibration of C═O bonds corresponding to non-ionic carboxyl groups (–COOH, $–COOCH_3$). These groups mainly originate from carboxylic acids or esters [26]. The wide band at 1054 cm^{-1} is related to stretching vibrations of C—O of alcohol groups and carboxylic acids. Carboxyl and hydroxyl groups in the structure of aLVB's surface are mainly in its deprotonated form which is of crucial importance for electrostatic attraction of metal ions from the solutions.

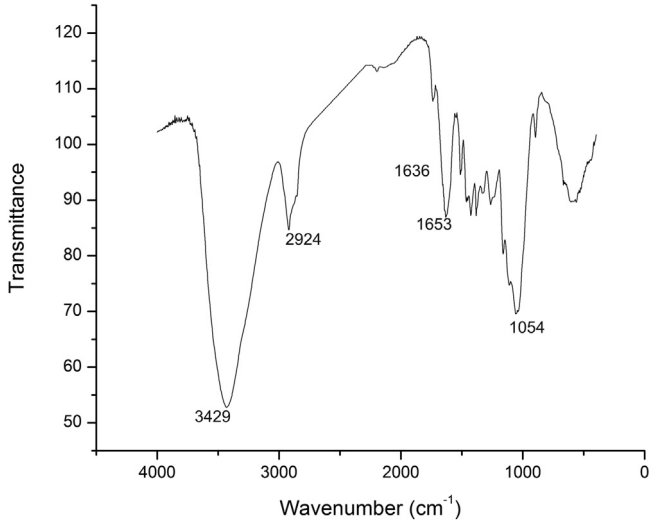

Fig. 1. FTIR spectrum of *Lagenaria vulgaris* biosorbent.

3.2. Morphological characterization of the aLVB (SEM and EDX)

Morphological characteristics of the *Lagenaria vulgaris* biosorbent before and after sorption of strontium ions from solutions are presented in Fig. 2. Generally, there is no major influence of sorption onto morphology on the biosorbent's particles. The dimensions, basic shape and edges of an inherent crispy-like structures of the biosorbent's grains are in comparable range before and after sorption. However, after taking a closer look, it is noticed that sorption of Sr(II) probably influenced the changes in the structure of the hollow shell-like formations on the biosorbent's surface. Namely, at initial concentration of the sorbate of 50 mg dm^{-3}, and even more at 400 mg dm^{-3}, certain extent of the cleavage and structural collapse of the shell openings is evident. This virtually decreases the number of hollow shells after the sorption. This phenomenon is probably related to the breaking of hydrogen bonds which link cellulose layers on the surface of a aLVB grains, supposedly triggered by sorption of Sr(II) ions.

Chemical analysis of LV which reveals its macromolecular, ash and moisture content was explained elsewhere and briefly presented in Table 1 (Ref. [27]). It simply elucidates the potential of this natural material for successful carbonization which would result in derivates of high surface areas and diverse surface functionality.

Weight ratios of carbon, oxygen and strontium before and after sorption processes were determined by the EDX. The results are presented in Table 2. Comparable ratios of carbon and oxygen are detected for all three samples, which is expected. EDX analysis also confirmed presence of strontium on the surface of sorbent after the treatment of model solutions. Strontium content is relatively similar in samples loaded with initial concentrations of 50 and 400 mg dm^{-3}. Increase of the amount of strontium obviously does not follow initial concentration of the metal, but this is typical for EDX technique when it is used for analysis of samples with irregular shape and porous surface. Anyway, presence of strontium on the samples of the sorbent after loading is evident.

3.3. pH_{PZC}

By using pH drift method for determination of pH_{pzc}, it was shown that pH at which surface of aLVB biosorbent is electroneutral is 6.46. Theoretically, it means that below this value surface of the material in the solution is positively charged, while above this value it is negatively charged. This assertion could be related to phenomena of electrostatical repulsions and attractions between the biosorbent's surface and Sr(II) ions from solution.

3.4. Boehm's titrations

Boehm's titrations were used herein to determine the acid-base character of aLVB and therefore estimate the types of electrical charges on the surface of aLVB and its origin which is generally crucial for sorption by ionic exchange. It was concluded that mainly strong acidic groups are present on the surface of aLVB. Concentration of carboxylic groups is 0.275 mmol g^{-1} while the concentrations of lactones and phenols are 0.160 and 0.295 mmol g^{-1}, respectively. These functional groups are probably to a great extent charged in wide range of pH values which is considered as the main factor in ion exchange. As previously stated, these acidic groups are protonated and positively charged in highly acidic and deprotonated and negatively charged in basic medium. This fact explains higher sorption capacities at higher pH values due to electrostatic attraction of negatively charged surface of aLVB and positively charged strontium ions.

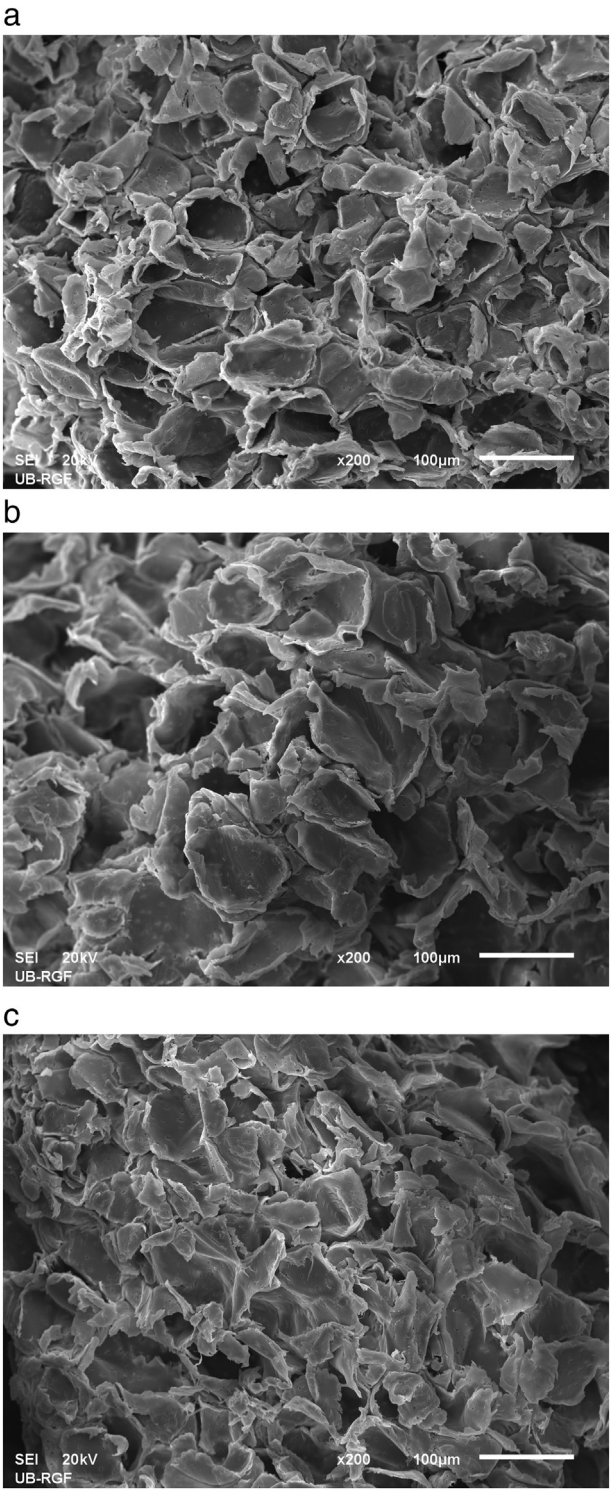

Fig. 2. SEM images of aLVB: a) before sorption b) after sorption 50 mg dm^{-3} of Sr(II) and c) after sorption 400 mg dm^{-3} of Sr(II).

Table 1
Chemical composition of aLVB.

Parameter	Values (%)
Cellulose	54.8
Lignin	40.3
Ash	0.28
Moisture	3.80

Table 2
Elemental content before and after sorption of Sr(II) from solution.

Sample	Carbon (%)	Oxygen (%)	Strontium (%)
aLVB – before sorption	53.1	46.6	/
aLVB – after sorbing 50 mg dm^{-3} Sr(II)	52.7	46.8	0.54
aLVB– after sorbing 400 mg dm^{-3} Sr(II)	52.5	47.1	0.46

3.5. Sorption of Sr(II)

3.5.1. Effects of contacting time

The effects of contacting time on the sorption of Sr(II) onto aLVB was investigated in the intervals 0, 1, 2, 4, 10, 20, 40, 60, 90, 120 and 240 min with all other parameters held constant (initial strontium concentration 50 mg dm^{-3}; pH 5; sorbent dose 4 g dm^{-3}). The dependence of sorption capacity (q_t) and corresponding time interval is given in Fig. 3.

Sorption rate of metal uptake was very fast and decreased with increasing of contacting time. In the beginning of the process, a strong concentration gradient leads to a fast sorption rate. Sorption capacity reaches about 9.5 mg g^{-1} within the first 4 min. After that time, the rate of sorption is reduced. This phenomenon relates to the availability of the active sites on the sorbent's surface and high sorption capabilities. The sorption becomes less efficient and reaches a constant value with gradual occupying of the active sites [28]. Sorption equilibrium was reached after about 10 min (with q_t of about 12 mg g^{-1}) and further increase in contacting time did not show significant increase of sorption since the concentration gradient decreases.

3.5.2. Effects of pH

The pH value is one of the most important factors for sorption processes since it affects both the sorbent and the ionic state of the sorbate [29]. Hydrolysis constant of Sr(II) determines that in the pH range from 1 to 11 the strontium in solution can exist in the form of Sr^{2+} while at pH > 12 $Sr(OH)^{+}$ becomes predominant [30]. Herein, the effects of pH on the sorption of Sr(II) onto aLVB were studied at pH 2, 3, 4, 5, 6, 7, 8, 9 and 10 while other conditions were kept constant. Fig. 4 shows dependence of sorption capacity with pH for constant initial concentration of Sr(II) (50 mg dm^{-3}) and sorbent dose of 4 g dm^{-3}.

The results in the Fig. 4 show that at pH 2 and 3, there was no significant removal of the Sr(II) ions since sorption capacity was only about 2 mg g^{-1}. The increase of pH from 3 to 7 causes a rapid increase in

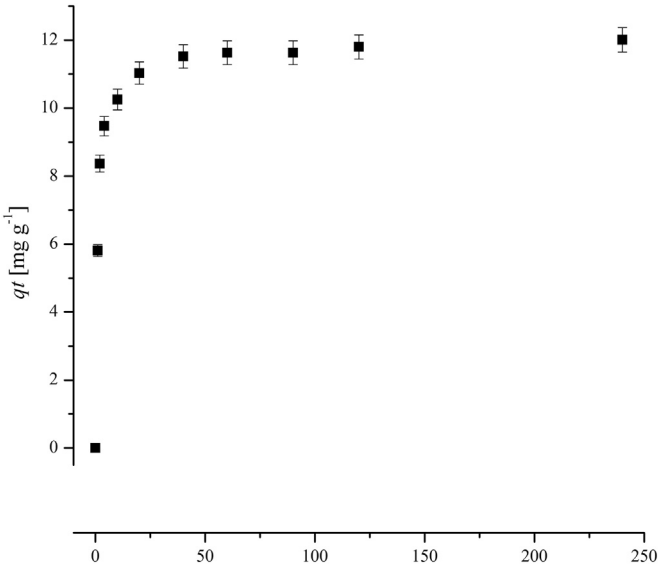

Fig. 3. Effects of contacting time on the sorption of Sr(II) onto aLVB (error bars represent ±SD).

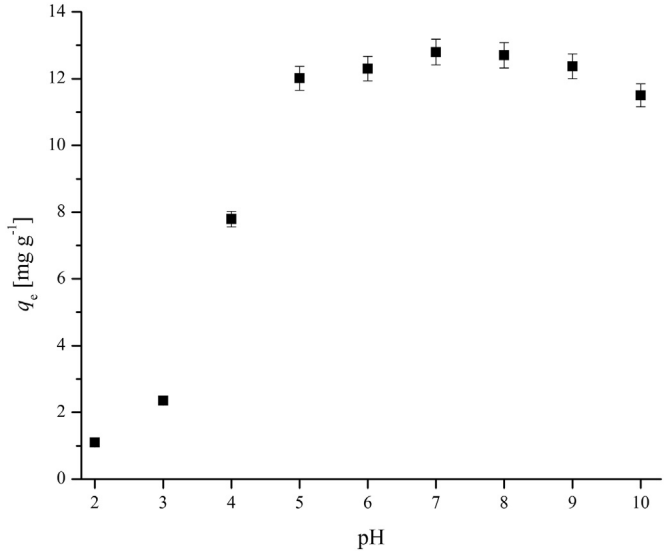

Fig. 4. Influence of pH on the sorption of Sr(II) onto aLVB (error bars represent ±SD).

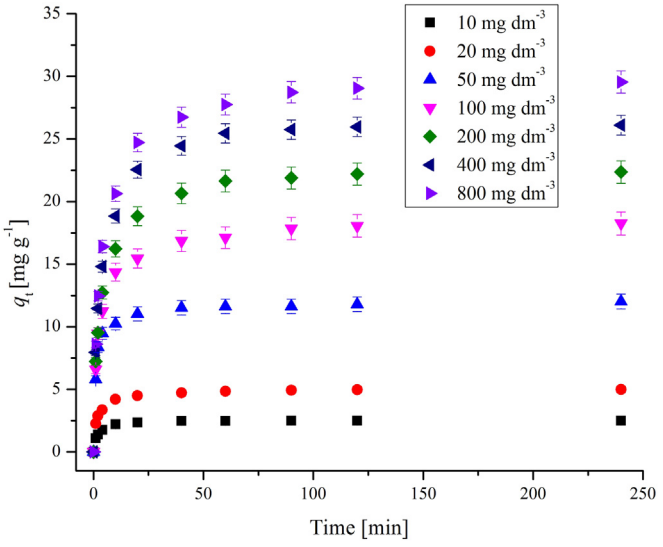

Fig. 5. Effects of initial Sr(II) concentration on sorption onto aLVB (error bars represent ± SD).

biosorption capacity. With pH increase after 7, removal of strontium starts to decrease. It is speculated that, for the sorbents which possess carboxyl and other groups such as carbonyl, hydroxyl ane phenyl functional groups, cation exchange is the main mechanism of sorption and removal of cations from aquaeous solutions [31]. At pH values lower than 5, hydrogen ions would compete with metal cations to be sorbed onto the mentioned functional groups of the sorbent. For the present case of Sr(II) removal and pKa 4.8, the following mechanism is expected:

$$\left[(-\mathrm{COO})_n\mathrm{Sr}\right]^{(2-n)+} + n\mathrm{H}^{+1} \leftrightarrow n\mathrm{COOH} + \mathrm{Sr}^{2+}\ (n = 1, 2)$$

Thus, high acidity results in replacement of sorbed Sr(II) ions by H^+ and decreasing of the sorption capacity. By increasing the pH, metal ions in solution will compete with less H^+ ions for sorption sites and consequently bind in higher degree [32]. At high pH range [8–10] sorption capacity partially decreases. One of the main reasons for this could be partial transformation of Sr(II) ions to hydroxy forms, $Sr(OH)^+$ and $Sr(OH)_2$ [33], which cannot be sorbed as free ionic strontium [34]. The increase of sorption capacity is negligible with increase of pH from 5 to 7. Therefore, pH value 5 was used in the later studies.

3.5.3. Effects of initial Sr(II) ion concentration

The effects of initial metal concentration were investigated for 10, 20, 50, 100, 200, 400 and 800 mg dm^{-3}, while other conditions were kept constant. Kinetics for different initial concentrations is given in Fig. 5.

Graph in Fig. 5 shows that sorption capacity for Sr(II) increases with increase of its initial concentration. These results may be explained by the fact that initial metal concentration provides a driving force to overcome all mass transfer resistances between the biosorbent and biosorption medium [35]. It is evident that in all cases and for all initial concentrations the greatest pick-up in sorption capacity is attained within a few minutes after the introduction of aLVB into the solution of strontium. After this, a mild increase in time is noticed especially for lower initial concentrations. The fact that sorption equilibrium was reached in 60 min (for high initial concentrations), indicates that the material has poor porosity.

3.5.4. The effects of biosorbent's loading

Fig. 6 depicts the influence of sorbent's dosage on strontium removal efficiency expressed in percentage. The removal efficiency of Sr(II) was increased with increasing of biosorbent dose. Significant rise of sorption efficiency is noticeable above the aLVB dosage of 4 g dm^{-3}. This phenomenon is simply explained by increasing the amount of active sorption cites with increasing sorbent dose. As previously stated, this cites are mainly related to charged carboxyl, hydroxil, lactonic and other acidic functional groups responsible for ionic exchange. It was determined that optimal dosage was 4 g dm^{-3}. This value corresponds to the case where all active sites on the sorbent's surface are occupied in the best geometrical and energetic manner. Further increase in sorbent's dose leads to some decrease of sorption capacity and removal efficiency probably due to the increase of diffusion resistance i.e. because of the resistance to mass transfer, as shown in Fig. 6.

3.6. Kinetic modelling

The chemical kinetics elucidates reaction pathways along times to reach the equilibrium, whereas chemical equilibrium gives no information about pathways and reaction rates. Sorption kinetics shows a large dependence on the physical and chemical characteristics of the sorbent material, which also influences the sorption mechanism. In our study, several theoretical kinetic models were used to investigate the mechanism of the sorption at different experimental conditions including

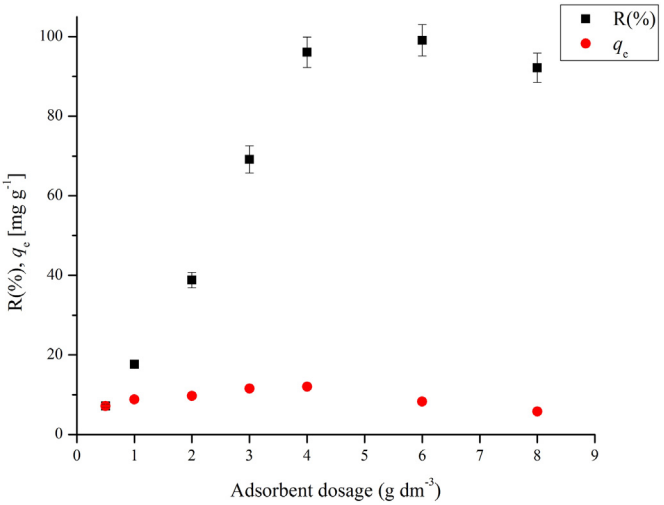

Fig. 6. Effects of sorbent's loading onto Sr(II) removal (error bars represent ± SD).

pseudo-first and pseudo second order, intraparticle diffusion and Chrastil kinetic models. The best fitting model was selected based on the coefficient of determination values (r^2) determined after non-linear regression analysis in software OriginPro 2016 (OriginLab Corporation, USA).

The pseudo first-order model defined by Lagergren is represented by the equation given as:

$$q_t = q_e\left(1-e^{-k_1 t}\right) \tag{5}$$

where q_e and q_t (mg g^{-1}) are the amounts of sorbed Sr(II) ions on the biosorbent at equilibrium and at time t, respectively, while K_1 is the first-order biosorption rate constant (min^{-1}). In most cases, the first-order equation does not fit well over the entire sorption period and it is generally applicable over the initial 30 to 50 min from the onset of the experiment [36].

Pseudo second-order model, on the other hand, includes the behavior over the whole time of the contacting. The pseudo second-order rate equation is expressed as in the reference [37]:

$$\frac{t}{q_t} = \frac{1}{K_2 q_e^2} + \frac{1}{q_e} t \tag{6}$$

where K_2 is the second-order biosorption rate constant (g mg^{-1} min), q_e is the biosorption capacity at the equilibrium (mg g^{-1}).

Intraparticle diffusion equation was introduced to draw attention to the processes of diffusion inside the particles of sorbent as the rate-limiting step. This model is described by the following equation [38]:

$$q_t = k_t\sqrt{t} \tag{7}$$

where q_t is the amount of sorbed Sr(II) ions at time t and K_s is the intraparticle diffusion constant.

Finally, Chrastil's model was analyzed. Its equation is given as [39]:

$$q_t = q_e\left(1 = e^{-k_C A_0 t}\right)^n \tag{8}$$

where: k_c is the rate constant (dm^3 g^{-1} min^{-1}), which depends on diffusion coefficients and sorption capacity of biosorbent, A_0 is dose of biosorbent (g dm^{-3}) and n is the heterogeneous structural diffusion resistance constant, which can range from 0 to 1. When diffusion resistance is small, n tends to be 1 and the reaction is of the first order. If the system is strongly limited by diffusion resistance, n value is small. In addition, when $n > 1$, consecutive reaction order may be expected [34].

The applicability of the pseudo first-order, pseudo second-order, interparticle diffusion and Chrastil model was tested for a different initial Sr(II) ion concentration as it can be seen in Table 3.

The pseudo-first order model is valid only in cases where biosorption process occurs rapidly and considers the rate of occupation of biosorption sites to be proportional to the number of unoccupied sites. As the initial ion concentration increases, r^2 value decreases. When ion concentration is lower, the process is very fast, because there are enough active centers to be occupied. It was observed that the rate constants decreased gradually with increasing of concentration, indicating that the increase in driving force caused by higher Sr(II) concentration influences the rate of removal during the first minutes of contacting. The theoretic values of q_e are lower than the corresponding experimental data q_e, whereby the difference rises with concentration, indicating that the sorption process does not fully provide the pseudo-first order sorption rate expansion.

The results given in Table 3 indicate that the coefficients of determinations for the pseudo second-order were higher than 0.99 for all the cases, while theoretical q_e values also were compatible with experimental data in the whole range of initial Sr(II) concentration. It can also be seen that the equilibrium sorption capacity (q_e) increases as the initial Sr(II) concentration (c_i) increases. This suggests that the pseudo-second-order model well describes sorption process. This model is based on the assumption that the rate-controlling step in the sorption process depends on both, initial concentration of Sr(II) ions and the number of unoccupied sites at sorbent's surface. Also, the pseudo-second-order model indicates that the mechanism of sorption process is probably based on chemisorption and ion exchange.

The values of parameters for the Chrastil's model, based on Eq. (8) determined by non-linear regression are shown in Table 3. The coefficients of determinations (r^2) in all cases are very high and amount $r^2 >$ 0.99. In all the cases, theoretical q_e values fit well with experimental data. The values of diffusion resistance coefficient (n) for all initial

Table 3
Parameters of kinetics modelling for biosorption of Sr(II) onto aLVB.

Parameters	10 [mg dm^{-3}]	20 [mg dm^{-3}]	50 [mg dm^{-3}]	100 [mg dm^{-3}]	200 [mg dm^{-3}]	400 [mg dm^{-3}]	800 [mg dm^{-3}]
q[mg g^{-1}] (experiment)	2.50	4.50	12.01	18.25	22.36	26.10	29.55
Pseudo-first order							
k_1 [min^{-1}]	0.415	0.451	0.644	0.348	0.252	0.244	0.237
q_e^{cal}[mg g^{-1}]	2.43	4.72	11.33	16.91	20.94	24.67	27.37
r^2	0.970	0.949	0.972	0.948	0.947	0.952	0.948
Pseudo-second order							
k_2 [g mg^{-1} min^{-1}]	0.256	0.140	0.088	0.028	0.016	0.013	0.011
q_e^{cal}[mg g^{-1}]	2.53	4.93	11.77	17.85	22.27	26.22425	29.17
r^2	0.996	0.992	0.995	0.991	0.991	0.993	0.992
Chrastil model							
q_e^{cal}[mg g^{-1}]	2.49	4.92	11.63	17.79	22.06	25.82	28.86
n	0.383	0.280	0.290	0.310	0.360	0.386	0.370
k_c [dm^3 g^{-1} min^{-1}]	0.031	0.019	0.035	0.015	0.013	0.015	0.013
r^2	0.999	0.997	0.986	0.993	0.998	0.998	0.996
Intraparticle diffusion model							
K_{id1} [mg g^{-1} $min^{-0.5}$]	0.885	1.730	4.927	5.789	5.112	5.969	5.352
C_1	0.081	0.223	0.475	0.434	1.397	1.564	3.056
r^2	0.967	0.933	0.944	0.966	0.944	0.942	0.919
K_{id2} [mg g^{-1} $min^{-0.5}$]	0.081	0.138	0.474	0.622	1.151	0.889	0.795
C_2	1.971	3.818	8.677	12.572	13.091	18.655	21.414
r^2	0.981	0.942	0.933	0.930	0.930	0.980	0.960

concentrations are in the range from 0.28 to 0.39, which indicates that the sorption process of Sr(II) ions onto aLVB is significantly limited by diffusion resistance.

The intraparticle diffusion model also shows good agreement with the experimental results (Table 3). The coefficients of determinations (r^2) for the intraparticle diffusion model are between 0.92 and 0.98. The initial curved portions might be attributed to the boundary layer diffusion effects, while the final linear portions might be due to intraparticle diffusion effects. In addition, the values of K_{id1} obtained from the intra-particle diffusion model are higher for the first stage than for the second stage (K_{id2}), indicating that, as expected, the rate of sorption is faster at the beginning of the experiment. As the initial concentration of Sr(II) ions is increased, the amount of Sr(II) ions that reach the surface of sorbent increases as well, therefore the intraparticle diffusion rate increases, i.e. the film diffusion rate is large enough and the intraparticle diffusion is a rate-controlling process. The values of C give an insight about boundary layer thickness: when the value of the intercept is larger, the boundary effect is greater. The increasing of C values with initial Sr(II) concentration indicates the growing thickness of the boundary layer. The increase in boundary layer thickness (larger value of the intercept, C), would decrease the external mass transfer thus increasing the chance of internal mass transfer.

3.7. Isotherm modelling

Sorption isotherms describe the relationship between the mass of the sorbed matter per unit mass of biosorbent and the concentration of this matter in the solution. Determination of equilibrium parameters provides important information useful for the design of sorption processes.

In this study, Langmuir, Freundlich, Temkin, Sips, Brouers-Sotolongo and Dubinin-Radushkevich isotherm models were applied. These models are simple, well-established and easy to interpret, which explains their frequent and extensive use. All the experimental data given in the form that suits a certain model is on the corresponding graph fitted nonlinearly in order to determine, so called, best fit. The validity of the model is verified by the coefficients of determination (r^2) which are determined by the fittings in software OriginPro 2016 (OriginLab Corporation, USA).

The Langmuir isotherm equation is valid for monolayer sorption onto surface containing a finite number of identical sorption sites. It means that all of the sorption centers have the same binding energy. The Langmuir isotherm equation is represented by the following equation [40]:

$$q_e = \frac{q_m K_L c_e}{1 + K_L c_e} \tag{9}$$

where c_e is the equilibrium concentration of sorbate in the solution (mg dm^{-3}), q_m the monolayer sorption capacity of the sorbent (mg g^{-1}), and K_L is the Langmuir biosorption constant (dm^3 mg^{-1}) which is related to the free energy of biosorption.

R_L as a dimensionless separation factor is showing the affinity between Sr(II) ions and the sorbent aLVB, which can be defined by equation:

$$R_L = \frac{1}{1 + K_L c_i} \tag{10}$$

The separation factor (R_L) values indicate the type of the isotherm and may be unfavorable ($R_L > 1$), linear ($R_L = 1$), favorable ($0 < R_L < 1$), and irreversible ($R_L = 0$). The R_L values were calculated for initial Sr(II) ions concentrations from 10 to 800 mg dm^{-3}.

The Freundlich isotherm is an empirical model used to describe sorption onto heterogeneous systems. The Freundlich equation is given as [41]:

$$q_e = K_F c_e^{1/n} \tag{11}$$

where K_F (dm^3 g^{-1}) and n are Freundlich sorption isotherms constants. $1/n$ values indicate the type of isotherm to be irreversible ($1/n = 0$), favorable ($0 < 1/n < 1$) and unfavorable ($1/n > 1$).

This empirical model can be applied to non-ideal sorption onto heterogeneous surfaces as well as in cases where multilayer sorption takes place.

The Temkin isotherm model shows that the heat of sorption of all the molecules in the layer decreases linearly with coverage area due to sorbent-sorbate interactions. The Temkin isotherm is expressed as [42]:

$$q_e = \frac{RT}{b_T} \ln(K_T c_T) \tag{12}$$

where Temkin constant K_T (dm^3 mg^{-1}) is the equilibrium binding constant which correlates with the maximum binding energy; R is universal gas constant (8.314 J mol^{-1} K^{-1}); T (K) is absolute temperature and b_T (J mol^{-1}) is related to heat of sorption.

Sips isotherm is a combined form of Langmuir and Freundlich isotherms deduced for predicting the heterogeneous sorption systems. At low sorbate concentrations, it is reduced to Freundlich isotherm, while at high concentrations (n close to 1), it predicts a monolayer sorption capacity characteristic for the Langmuir isotherm [43,44]. It is originally given as:

$$q_e = \frac{q_m (b_S c_e)^n}{1 + (b_S c_e)^n} \tag{13}$$

where q_m is the maximum sorption capacity of the sorbent (mg g^{-1}), b_S (dm^3 mg^{-1}) is Sips equilibrium constant (which is related to sorption affinity), while n_S is exponential factor with values between 0 and 1.

The Brouers-Sotolongo isotherm is given by a deformed exponential (Weibull) function as [45]:

$$q_e = q_m \left(1 - e^{\left(-K_W C_e^a\right)}\right) \tag{14}$$

where q_m is the saturation value (mg g^{-1}); K_w is the model constant (dm^3 mg^{-1}) and the exponent α is a measure of the width of the

Table 4
Equilibrium model parameters for sorption of Sr (II) onto aLVB.

Isotherm	Calculated parameters						r^2
Langmuir	q_m [mg g^{-1}]	25.15	K_L [dm^3 mg^{-1}]	0.367	R_L [/]	0.214–0.003	0.854
Freundlich	K_F [dm^3 g^{-1}]	10.29	n [g dm^{-3}]	6.108			0.996
Temkin	K_T [dm^3 mg^{-1}]	904.49	B [Jmol^{-1}]	1.998			0.942
Sips	q_m [mg g^{-1}]	80.42	b_S [dm^{-3} mg^{-1}]	0.147	n_S	0.209	0.999
Brouers-Sotolongo	q_m [mg g^{-1}]	52.72	K_W [(mg g^{-1}) (dm^3 mg^{-1})$^{1/\alpha}$]	0.217	a	0.203	0.999
Dubinin-Radushkevich	q_D [mg g^{-1}]	26.33	B_D [mol^2 J^{-2}]	1.68×10^{-9}	E [kJ mol^{-1}]	17.26	0.985

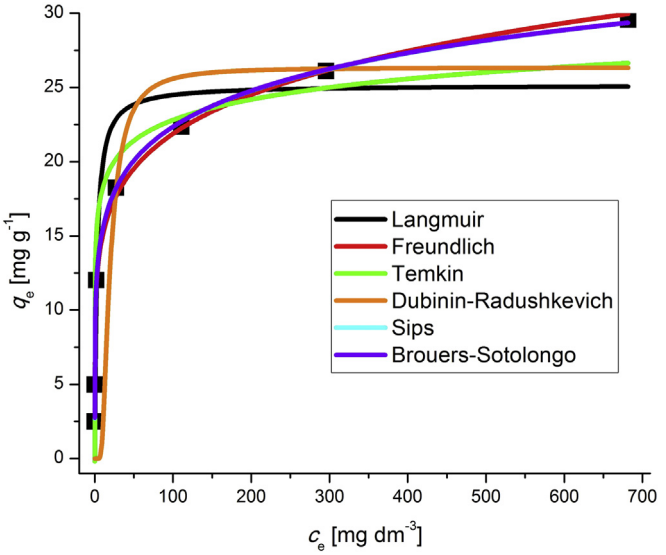

Fig. 7. Sorption isotherm fitted to theoretical models.

sorption energy distribution and therefore of the energy heterogeneity of the sorbent surface.

Dubinin-Radushkevich (D-R) model is expressed as:

$$q_e = q_D \exp\left(-B_D\left[RT \ln\left(1+\frac{1}{c_e}\right)\right]^2\right) \quad (15)$$

where q_D is the pore filling limit (mg g^{-1}), B_D is a fitting parameter related to the adsorption energy (mol^2 J^{-2}) and c_e is the molar equilibrium concentration of the solute (mol dm^{-3}) [46]. This model postulates a fixed volume close to the sorbent surface where sorption takes place and heterogeneity of sorption energies within this space [47].

The parameters obtained by fitting experimental data to the Langmuir, Freundlich, Temkin, Sips, Brouers-Sotolongo and Dubinin-Radushkevich models are compared in Table 4. Graph representing non-linear fitting to these models is given as Fig. 7. Dubinin–Radushkeveich model which implies expressing q_e in mmol g^{-1}, is included in this figure only symbolically in order to depict relative position of this fitting in comparison to the other models.

Generally, the differences between these models are reflected in the number of parameters to fit, taking account of a maximum monolayer sorption or not, and considering homogeneous or heterogeneous sorption. The Table 4 indicates that all the isotherm models gave reasonable fit to experimental data. It can be seen that Freundlich model gave the best fit to experimental data. Freundlich model defined the equilibrium experimental data more closely, as evidenced by r^2 values higher than in case of the Langmuir and Temkin isotherm model. The values of r^2 for Freundlich isotherm model are not the greatest. Sips and Brouers-Sotolongo isotherm models have the highest values for the coefficient of determination.

However, the values for the sorption capacity q_m obtained from the isotherm model of Sips and Brouers-Sotolongo are greater than the experimentally obtained values. The Freundlich model is basically empirical and was developed for heterogeneous surfaces. The results show that the value of n (Freundlich adsorption isotherms constants) is greater than a unit, indicating that Sr(II) ions are favorably sorbed by aLVB, which is in great agreement with R_L values obtained from Langmuir isotherm model. The high values for K_F and n are indication of high adsorption throughout the examined concentration range. The values of K_F in Freundlich model are related to the bond strength, which suggests strong affinity for sorption of Sr(II) ions onto aLVB.

The maximum sorption capacity obtained from the Langmuir isotherm model was close to the experimentally obtained values. The R_L values were calculated for initial Sr(II) ions concentrations from 10 to 800 mg dm^{-3}. R_L decreased from 0.214 to 0.003 as the initial concentration increased from 10 to 800 mg dm^{-3} showing that the reaction became more favorable at higher initial Sr(II) concentrations. However, the value of r^2 for the Langmuir model is quite low. As previously described, Sips is an integral model which incorporates functions of both Langmuir and Freundlich models. In cases of low sorbate concentrates, Sips model is reduced to Freundlich model which is herein explain by good fitting to both models. Fitting of Sips model is as seen on Fig. 7 overlapped probably by fitting to the Freundlich model. This in any case implies that the surface of the sorbent is heterogenous and

Table 6
Sorption and desorption of Sr(II) onto aLVB in batch cycles.

Desorption agent	Number of cycles	Uptake capacity (mg dm^{-3})	Desorption efficiency (%)
HNO_3 (0.1 M)	1	11.95	99.25
	2	11.86	98.88
	3	11.64	98.24
	4	11.68	98.32
	5	11.62	97.76
	6	11.58	97.64
HCl (0.1 M)	1	11.98	99.45
	2	12.02	99.38
	3	11.91	99.24
	4	11.88	99.32
	5	11.82	98.96
	6	11.74	98.94
NaCl (0.1 M)	1	11.94	15

Table 5
Comparison of Sr(II) sorption onto various biosorbents.

Biosorbent	Experimental conditions	q_{max} (mg g^{-1})	Source
Native peanut husk	c_i = 10–100 mg dm^{-3} dosage = 4 g dm^{-3}	9.4	Ref. 49
Chitosan	c_i = 5–300 mg dm^{-3} dosage = 2 g dm^{-3}	81.96	Ref. 50
Aerobic granules	c_i = 10–160 mg dm^{-3} dosage = 1.7 g dm^{-3}	28.8	Ref. 51
Amaranthus spinosus root	c_i = 25–400 mg dm^{-3} dosage = 4 g dm^{-3}	12.89	Ref. 52
Fe_3O_4 particles modified sawdust	c_i = 5–50 mg dm^{-3} dosage = 0.4–5 g dm^{-3}	12.59	Ref. 53
Moss biosorbent	c_i = 0–2500 mg dm^{-3} dosage = 0.625–18.75 g dm^{-3}	38	Ref. 22
Lagenaria vulgaris shell	c_i = 10–800 mg dm^{-3} dosage = 4 g dm^{-3}	29.55	This study

probably involves sorption in more than one layers where strontium ions are sorbed with different binding energies.

The Temkin isotherm model indicates that the sorption is characterized by a uniform distribution of binding energies, up to some maximum binding energy and that the heat of sorption decreases linearly with coverage due to sorbent-sorbate interactions. In the case of aLVB, the values of the coefficients of Temkin isotherm i.e. K_T and B were 904.49dm^3 mg^{-1} and 1.998 J mol^{-1}, respectively. The value of r^2 in Temkin isotherm model was lower than those in the Freundlich, Sips and Brouers-Sotolongo isotherms, thus suggesting that it was inappropriate in explaining the sorption mechanism in the present case. The value for the bonding energy was <8 kJ mol^{-1} which implies physical sorption.

Brouers-Sotolongo isotherm model has a high value for coefficient of determination, which indicates the presence of active sites with heterogeneous sorption interactions. Based on α (being related to the heterogeneity, $\alpha < 1$) it can be inferred that the sorption environment in aLVB material was heterogeneous. The heterogeneous surface as a consequence of differences in size of pores and different functional groups (carboxyl, hydroxil, lactonic and other acidic functional groups) shows that the Sr(II) ions sorption onto aLVB is a complex process. This suggests that the mechanism of sorption between Sr(II) onto aLVB occurs via different possible interactions: chemisorption and ion exchange.

Dubinin-Radushkevich model gave also a good fit. This model's parameter q_D, which indicates the pore filling limit, was consistent with the Langmuir adsorption isotherm model parameter q_m, indicating the monolayer surface coverage limit. Estimated bonding energy by this model is 17.26 kJ mol^{-1}. The typical range of bonding energy for ion-exchange mechanisms of divalent metal ions is 8–16 kJ mol^{-1} which corresponds well to our case [48].

The Gibbs free energy (ΔG°) was calculated from the Freundlich isotherms by using adsorption isotherm constant (K_F) in the calculations. The free energy change of the sorption reaction was calculated from the Van't-Hoff equation and showed by the following equation:

$$\Delta G^\circ = -RT \ln K_F \quad (16)$$

where ΔG° is standard free energy change (J); R the universal gas constant, 8.314 J mol^{-1} K^{-1}; T is the absolute temperature (K); and K_F is the equilibrium constant obtained from the Freundlich isotherm model for sorption Sr(II) ions onto aLVB. The obtained value for ΔG° was −5.68 kJ mol^{-1}. The negative ΔG° value suggests that sorption Sr (II) ions onto aLVB were of spontaneous nature and feasible.

Table 5 (references [22, 49–53]).

Comparison of Sr(II) sorption onto several different biosorbents where similar approach and experimental conditions were applied is given in Table 5. It is noticeable that LV biosorbent expressed interesting potential among the rest of the materials especially in the sense of cost of plant cultivation, sorbent preparation, and its application in described manner.

The reusability (i.e. regeneration) of biosorbent is very important for the potential application of sorption technology. Herein, batch desorption studies were conducted using three different eluting agents: two acids (HCl and HNO_3) and one salt (NaCl).

The results presented in Table 6 show that both applied acids are very good desorption agents since >97.5% desorption recovery was obtained in six adsorption–desorption cycles. This indicates that sorption process involves ion exchange as previously postulated.

aLVB exerted good adsorption capacity for Sr(II) even after six cycles. The total decrease in sorption capacity of aLVB for Sr(II) after six cycles was less than 3%, which shows that aLVB has good potential for repeated use in strontium removal from aqueous solutions.

Also, considering that almost all amount of metal ions were removed from aLVB after desorption, it is possible to carry out an efficient recovery of polluting agent from desorbing solution. Desorbed Sr(II) ions can be separated from preconcentrated acid solution and separated by chemical precipitation or some other method.

Contrary to acids, desorption of Sr(II) ions using NaCl solution was almost negligible with DE of only 15%. This could be important for removal of Sr(II) ions from the seawater where concentration of NaCl is about 3.5%.

4. Conclusion

The biosorbent prepared from the shell of the *Lagenaria vulgaris* plant showed significant potential in strontium removal from model aquaeous solutions. Characterization of this biomaterial reveled abundance of acidic (carboxyl and hydroxyl) functional groups on its surface. These groups are charged at any pH value except on 6.46 which is determined to be pH_{pzc}. In accordance with this, boost of sorption efficiency in basic conditions is coherent with electrostatic attractions of negatively charged biosorbent's surface and positively charged Sr(II) ions. Investigation of sorption kinetics evidenced swift reaching of equilibrium after only 10 min, following the pseudo-second-order and the Chrastil's models. Good fitting to both Freundlich and Sips models implies presence of active binding sites in the structure of aLVB which sorb strontium ions with different energies. Maximal sorption capacity of 29.55 mg g^{-1} pronounced large potential of aLVB for strontium removal from aquaeous solutions. Mild alterations in sorbent's morphology are noticed after the sorption. In desorption study, aLVB retained good adsorption capacity for Sr(II) even after six cycles when acidic desorbents were used. To conclude, in this study, notable sorptive potential of sorbent based on LV plant toward Sr(II) ions is examined and presented in useful and comparable manner which deserves further economic estimations in terms of certain practical exploitation and applications.

Acknowledgement

Financial support from the Serbian Ministry of Education, Science and Technological Development through the framework of the project (TR 34008) is gratefully acknowledged.

References

[1] T.A. Todd, T. Batcheller, J.D. Law, R.S. Herbst, Cesium and strontium separation technologies literature review, INEEL/EXT-04-01895. Idaho, 2004.
[2] S.V. Avery, Fate of caesium in the environment: distribution between the abiotic and biotic components of aquatic and terrestrial ecosystems, J. Environ. Radioact. 30 (2) (1996) 139–171.
[3] M.G. Marageh, S.W. Husain, A.R. Khanchi, Selective sorption of radioactive cesium and strontium on stannic molybdophosphate ion exchanger, Appl. Radiat. Isot. 50 (1999) 459–465.
[4] M. Sasmaz, A. Sasmaz, The accumulation of strontium by native plants grown on Gumuskoy mining soils, J. Geochem. Explor. 181 (2017) 236–242.
[5] C.P. Lee, Y.M. Kuo, S.C. Tsai, Y.Y. Wei, S.P. Teng, C.N. Hsu, Numerical analysis for characterizing the sorption/desorption of cesium in crushed granite, J. Radioanal. Nucl. Chem. 275 (2008) 343–348.
[6] B. Onghena, C.R. Borra, T. Van Gerven, K. Binnemans, Recovery of scandium from sulfation-roasted leachates of bauxite residue by solvent extraction with the ionic liquid betainium bis(trifluoromethylsulfonyl)imide, Sep. Purif. Technol. 176 (2017) 208–219.
[7] Z. Majidnia, M.A. Fulazzaky, Photocatalytic reduction of Cs(I) ions removed by combined maghemite-titania PVA-alginate beads from aqueous solution, J. Environ. Manag. 191 (2017) 219–227.
[8] V.A. Volkovich, T.R. Griffiths, R.C. Thied, Treatment of molten salt wastes by phosphate precipitation: removal of fission product elements after pyrochemical reprocessing of spent nuclear fuels in chloride melts, J. Nucl. Mater. 323 (2003) 49–56.
[9] E.D. Hwang, K.W. Lee, K.H. Choo, S.J. Choi, S.H. Kim, C.H. Yoon, C.H. Lee, Effect of precipitation and complexation on nanofiltration of strontiumcontaining nuclear wastewater, Desalination 147 (2002) 289–294.
[10] A.M. El-Kamash, M.R. El-Naggar, M.I. El-Dessouky, Immobilization of cesium and strontium radionuclides in zeolite-cement blends, J. Hazard. Mater. B136 (2006) 310–316.
[11] F. Jia, J. Li, J. Wang, Y. Sun, Removal of strontium ions from simulated radioactive wastewater by vacuum membrane distillation, Ann. Nucl. Energy 103 (2017) 363–368.

[12] S. Chegrouche, A. Mellah, M. Barkat, Removal of strontium from aqueous solutions by adsorption onto activated carbon: kinetic and thermodynamic studies, Desalination 235 (2009) 306–318.
[13] M.W. Munthali, E. Johan, H. Aono, N. Matsue, Cs+ and Sr2+ adsorption selectivity of zeolites in relation to radioactive decontamination, J. Asian Ceramic Soc. 3 (2015) 245–250.
[14] A.K. Vipin, S. Ling, B. Fugetsu, Sodium cobalt hexacyanoferrate encapsulated in alginate vesicle with CNT for both cesium and strontium removal, Carbohydr. Polym. 111 (2014) 477–484.
[15] I. Smičiklas, A. Onjia, S. Raičević, Experimental design approach in the synthesis of hydroxyapatite by neutralization method, Sep. Purif. Technol. 44 (2005) 97–102.
[16] L. Zhang, J. Wei, X. Zhao, F. Li, F. Jiang, M. Zhang, X. Cheng, Removal of strontium(II) and cobalt(II) from acidic solution by manganese antimonate, Chem. Eng. J. 302 (2016) 733–743.
[17] A. Ghaemi, M. Torab-Mostaedi, M. Ghannadi-Maragheh, Characterizations of strontium(II) and barium(II) adsorption from aqueous solutions using dolomite powder, J. Hazard. Mater. 190 (2011) 916–921.
[18] M. Liu, F. Dong, W. Zhang, X. Nie, S. Sun, H. Wei, L. Luo, S. Xiang, G. Zhang, Programmed gradient descent biosorption of strontium ions by Saccaromyces cerevisiae and ashing analysis: a decrement solution for nuclide and heavy metal disposal, J. Hazard. Mater. 314 (2016) 295–303.
[19] M. Asztemborska, M. Jakubiak, M. Rykaczewska, M. Bembenek, R. Stęborowski, G. Bystrzejewska-Piotrowska, Mycoextraction of radiolabeled cesium and strontium by *Pleurotus eryngii* mycelia in the presence of alumina nanoparticles: sorption and accumulation studies, J. Environ. Radioact. 164 (2016) 190–196.
[20] J. Marešová, M. Pipíška, M. Rozložník, M. Horník, L. Remenárová, J. Augustín, Cobalt and strontium sorption by moss biosorbent: modeling of single and binary metal systems, Desalination 266 (2011) 134–141.
[21] O. Chaalal, A.Y. Zekri, A.M. Soliman, A novel technique for the removal of strontium from water using thermophilic bacteria in a membrane reactor, J. Ind. Eng. Chem. 21 (2015) 822–827.
[22] J.P. Chen, Batch and continuous adsorption of strontium by plant root tissues, Bioresour. Technol. 60 (1997) 185–189.
[23] D.S. Decker-Walters, M. Wilkins-Ellert, S.M. Chung, J.E. Staub, Discovery and genetic assessment of wild bottle gourd [Lagenaria siceraria (Mol.) Standley, Cucurbitaceae] from Zimbabwe, Econ. Bot. 58 (2004) 501–508.
[24] V. Srivastava, P. Maydannik, M. Sillanpää, Synthesis and characterization of PPy@NiO nano-particles and their use as adsorbent for the removal of Sr(II) from aqueous solutions, J. Mol. Liq. 223 (2016) 395–406.
[25] D.L. Mitic-Stojanovic, A. Zarubica, M. Purenovic, D. Bojic, T. Andjelkovic, A. Bojic, Biosorptive removal of Pb2+, Cd2+ and Zn2+ ions from water by Lagenaria Vulgaris shell, Water SA 37 (2011) 303–312.
[26] F.T. Li, H. Yang, Y. Zhao, R. Xu, Novel modifed pectin for heavy metal adsorption, Chin. Chem. Lett. 18 (2007) 325–328.
[27] D.L. Mitic-Stojanovic, A. Zarubica, M. Purenovic, D. Bojic, T. Andjelkovic, A.Lj. Bojic, Biosorptive removal of Pb^{2+}, Cd^{2+} and Zn^{2+} ions from water by *Lagenaria vulgaris* shell, Water SA, 37(3) 303–312.
[28] A. Ahmadpour, M. Zabihi, M. Tahmasbi, T.R. Bastami, Effect of adsorbents and chemical treatments on the removal of strontium from aqueous solutions, J. Hazard. Mater. 182 (2010) 552–556.
[29] C. Chen, X. Wang, Sorption of Th(IV) to silica as a function of pH, humic/fulvic acid, ionic strength, electrolyte type, Appl. Radiat. Isot. 65 (2007) 155–163.
[30] Y. Chen, J. Wang, Removal of radionuclide Sr^{2+} ions from aqueous solution using synthesized magnetic chitosan beads, Nucl. Eng. Des. 242 (2012) 445–451.
[31] E.H. Rifi, F. Rastegar, J.P. Brunette, Uptake of cesium, strontium and europium by a poly(sodium acrylate acrylic-acid) hydrogel, Talanta 42 (1995) 811–816.
[32] V.J. Inglezakis, M.D. Loizidou, H.P. Grigoropoulou, Ion exchange of Pb^{2+}, Cu^{2+}, Fe^{3+}, and Cr^{3+} on natural clinoptilolite: selectivity determination and influence of acidity on metal uptake, J. Colloid Interface Sci. 261 (2003) 49–54.
[33] E. Oguz, Thermodynamic and kinetic investigations of PO_4^{3-} adsorption on blast furnace slag, J. Colloid Interface Sci. 281 (2005) 62–67.
[34] S. Skupiński, J. Solecki, Studies of strontium(II) sorption on soil samples in the presence of phosphate ions, J. Geochem. Exp. Dermatol. 145, 124–128.
[35] Lalhmunsiama, D. Tiwari, S.M. Lee, Physico-chemical studies in the removal of Sr(II) from aqueous solutions using activated sericite, J. Environ. Radioact. 147 (2015) 76–84.
[36] Z. Aksu, Equilibrium and kinetic modelling of cadmium(II) biosorption by C. Vulgaris in a batch system: effect of temperature, Biochem. Eng. J. 7 (2001) 79–84.
[37] M.Y. Arica, Y. Kacar, O. Genc, Entrapment of white-fungus Trametes versicolor in calginate beads: preparation and biosorption kinetic analysis for cadmium removal from an aqueous solution, Bioresour. Technol. 80 (2001) 121–129.
[38] F.C. Wu, R.L. Tseng, R.S. Juang, Initial behavior of intraparticle diffusion model used in the description of adsorption kinetics, Chem. Eng. J. 153 (2009) 1–8.
[39] J. Chrastil, Adsorption of direct dyes on cotton: kinetics of dyeing from finite baths based on new information, Text. Res. J. 60 (1990) 413–416.
[40] I. Langmuir, The adsorption of gases on plane surfaces of glass, mica and platinum, J. Am. Chem. Soc. 40 (9) (1918) 1361–1403.
[41] H.M.F. Freundlich, Over the adsorption in solution, J. Phys. Chem. 57 (1906) 385–471.
[42] M.I. Temkin, V. Pyzhev, Kinetics of ammonia synthesis on promoted iron catalyst, Acta Physica et Chimia USSR 12 (1940) 327–356.
[43] V.J.P. Vilar, C.M.S. Botelho, J.P.S. Pinheiro, R.F. Domingos, R.A.R. Boaventura, Copper removal by algal biomass: Biosorbents characterization and equilibrium modelling, J. Hazard. Mater. 163 (2–3) (2009) 1113–1122.
[44] R. Sips, On the structure of a catalyst surface, J. Chem. Phys. 16 (1948) 490–495.
[45] F. Brouers, O. Sotolongo, F. Marquez, J.P. Pirard, Microporous and heterogeneous surface adsorption isotherms arising from levy distributions, Physica A 349 (2005) 271–282.
[46] E. Nariyan, A. Aghababaei, M. Sillanpää, Removal of pharmaceutical from water with an electrocoagulation process; Effect of various parameters and studies of isotherm and kinetic, Sep. Purif. Technol. 188 (2017) 266–281.
[47] M. Akhtar, S.M. Hasany, M.I. Bhanger, S. Iqba, Low cost sorbents for the removal of methyl parathion pesticide from aqueous solutions, Chemosphere 66 (2007) 1829–1838.
[48] S.A. Al-Muhtaseb, M.H. El-Naas, S. Abdallah, Removal of aluminum from aqueous solutions by adsorption on date-pit and BDH activated carbons, J. Hazard. Mater. 158 (2008) 300–307.
[49] A. Kausar, G. MacKinnon, A. Alharthi, J. Hargreaves, H.N. Bhatti, M. Iqbal, A green approach for the Sr(II) removal from aqueous media: kinetics, isotherms and thermodynamic studies, Mol. Ther. (2017)https://doi.org/10.1016/j.molliq.2018.02.101.
[50] Y. Yin, J. Wang, X. Yang, W. Li, Removal of strontium ions by immobilized saccharomyces cerevisiae in magnetic chitosan microspheres, Nucl. Eng. Technol. 49 (2017) 172–177.
[51] L. Wang, C. Wan, D.J. Lee, J.H. Tay, X.F. Chen, X. Liu, Y. Zhang, Adsorption–desorption of strontium from waters using aerobic granules, J. Taiwan Inst. Chem. Eng. 44 (2013) 454–457.
[52] Jyh-Ping Chen, Batch and continuous adsorption of strontium by plant root tissues, Bioresour. Technol. 60 (1997) 185–189.
[53] Z. Cheng, Z. Gao, W. Ma, Q. Sun, B. Wang, X. Wang, Preparation of magnetic Fe3O4 particles modified sawdust as the adsorbent to remove strontium ions, Chem. Eng. J. 209 (2012) 451–457.